

# Parametric amplification of waves during gravitational collapse: a first investigation

Stanislav V. Babak<sup>1</sup> and Kostas Glampedakis<sup>1,2</sup>

<sup>1</sup> Department of Physics and Astronomy, Cardiff University, Cardiff CF2 3YB, United Kingdom

<sup>2</sup> Department of Mathematics, University of Southampton, Southampton SO17 1BJ, United Kingdom

E-mail: babak@astro.cf.ac.uk ; glampedakis@astro.cf.ac.uk

We study the dynamical evolution of perturbations in the gravitational field of a collapsing fluid star. Specifically, we consider the initial value problem for a massless scalar field in a spacetime similar to the Oppenheimer-Snyder collapse model, and numerically evolve in time the relevant wave equation. Our main objective is to examine whether the phenomenon of parametric amplification, known to be responsible for the strong amplification of primordial perturbations in the expanding Universe, can efficiently operate during gravitational collapse. Although the time-varying gravitational field inside the star can, in principle, support such a process, we nevertheless find that the perturbing field escapes from the star too early for amplification to become significant. To put an upper limit in the efficiency of the amplification mechanism (for a scalar field) we furthermore consider the case of perturbations trapped inside the star for the entire duration of the collapse. In this extreme case, the field energy is typically amplified at the level  $\sim 1\%$  when the star is about to cross its Schwarzschild radius. Significant amplification is observed at later stages when the star has even smaller radius. Therefore, the conclusion emerging from our simple model is that parametric amplification is unlikely to be of significance during gravitational collapse. Further work, based on more realistic collapse models, is required in order to fully assess the astrophysical importance of parametric amplification.

## I. INTRODUCTION

### A. A brief background

The gravitational collapse of stellar objects with mass over a certain threshold is known to produce one of the most spectacular events in Universe. Due to the release of an enormous amount of energy, collapse is one of most favourable sources for all kinds of electromagnetic observations. It is expected (or hoped) that the same will come true for gravitational wave observations, which are about to begin in the next few years with the completion of a network of interferometric detectors (for a recent review see [1]). A considerable amount of theoretical work (numerical in its majority) has been devoted to the description/prediction of the emitted gravitational waveform produced by such a catastrophic event (see for instance [2]). Despite this effort, great uncertainties still remain, mainly due to the unknown initial state of the collapsing body, the complexity of the physics involved in realistic collapse and the related excessive computational requirements.

The simplest general relativistic collapse model was introduced more than sixty years ago with the seminal work of Oppenheimer and Snyder (hereafter O-S) [3]. In that model the collapsing star is approximated as a freely falling “dust” fluid ball (see Section II for more details). Using the O-S model, Price [4] was the first to study the evolution of scalar field perturbations during spherically symmetric gravitational collapse, focusing on the last stages where a black hole is formed. Subsequent studies by Cunningham, Price and Moncrief [5] were extended to gravitational perturbations. It was found that, at the final stage of the collapse, the emitted waveform was dominated by the exponentially decaying quasinormal mode “ringing” of the newly born black hole. At even later times, the signal decayed as a power-law, representing radiation backscattered from the asymptotic gravitational field.

Collapse of relativistic polytropes was modelled by Seidel [6] (for a non-rotating configuration) and by Stark and Piran [7] (for an axisymmetric rotating configuration), who provided an estimate of the amount of energy released via gravitational radiation. In their calculations, the resulting waveform was mainly comprised of a short burst followed by the black hole ringdown. Recent efforts include the relativistic rotational core-collapse study of Dimmelmeier et.al. [8] and the more general investigation by Fryer et.al. [9]. We also refer the reader to the article of Font [10] (and references therein) where numerical techniques in general relativistic hydrodynamics are discussed.

## B. Motivation

In the present paper we aim to study a specific aspect of gravitational collapse that (to the best of our knowledge) has been overlooked in the literature, namely, the possibility of having parametrically amplified perturbations within the star. That such a process could operate, at least in principle, can be justified with the following argument.

It is well known that there is a qualitative similarity between the time-dependent gravitational field of a spherically symmetric collapsing star and the gravitational field of the closed Friedmann cosmological model. This similarity has been quantified in the celebrated O-S collapse model [3], which, despite its simplicity, gives reliable results. On the other hand, one of the most important results in the study of cosmological perturbations is that their interaction with the background gravitational field of the expanding Universe can lead to considerable amplification [11] (in addition to the overall “adiabatic” change  $\sim a^{-1}$ , where  $a$  is the cosmological scale factor). This mechanism is believed to be responsible for the immense amplification of tiny primordial gravitational quantum vacuum fluctuations and their promotion to classical fields, which are likely to have left measurable imprints in the CMB radiation observed today [12]. Moreover, these fields put a strong candidature for direct observation by the gravitational wave detectors [1].

Hence, based on the two points above, a natural question that arises is whether the gravitational field of a collapsing star could pump energy into perturbations (that can be of fluid or gravitational nature) temporary “living” inside the star. In this work we plan to give an answer to this question by considering the simplest possible model for a collapsing star. In particular, we keep those pieces of physics which are related to the phenomenon we try to study, and strip off unrelated features which might be a cause of technical problems and confusion. We shall adopt a collapse model which very closely resembles the known O-S model, but is even more simplified regarding the exterior to the star gravitational field (see next Section). In a realistic situation, we can think of a collapsing star as a generator of all kinds of perturbations (fluid, gravitational). In our toy model, this process is “mimiced” by placing some initial field inside the star and studying its subsequent evolution. Moreover, we are free to choose the time at which this field is first placed inside the star. Finally, another major simplification is to consider a massless scalar field as the perturbation. We expect, however, that our results can be extrapolated to the realistic case of gravitational perturbations. This claim is based on the work of Ford and Parker [13], where both scalar and gravitational perturbations in Friedmann spacetime were considered.

The remainder of the paper is organised as follows. In Section II we give a brief review of the O-S collapse model (subsection IIA) and subsequently discuss the properties of the scalar wave equation in the field of a collapsing star and of full Friedmann spacetime (subsection IIB). In subsection IIC we introduce our simplified collapse model. Section III is devoted to our numerical results (time-evolutions). Analytical calculations regarding the amount of amplification in terms of the field’s energy, are presented in Section IV. Section V offers a physical insight into the results of the previous Sections. Finally, a concluding discussion can be found in Section VI. Two Appendices are devoted to some technical details. Throughout the paper we have adopted geometrised units  $c = G = 1$ .

## II. A TOY-MODEL FOR GRAVITATIONAL COLLAPSE

### A. The Oppenheimer-Snyder model

We set off by giving a brief review of the standard O-S model (for a detailed presentation see [14]). In this model, the spacetime of a collapsing, spherically symmetric, pressureless, homogeneous fluid “ball” is constructed by patching together a piece of Schwarzschild geometry (describing the vacuum outside the star) and a piece of closed ( $k = +1$ ) Friedmann geometry (describing the stellar interior). The two metrics are matched smoothly across the surface of the star. Explicitly, the interior metric is written in familiar comoving coordinates  $(\eta, \chi, \theta, \phi)$ ,

$$ds^2 = a^2(\eta)[-d\eta^2 + d\chi^2 + \sin^2 \chi(d\theta^2 + \sin^2 \theta d\phi^2)] \quad (1)$$

while the exterior metric is, in Schwarzschild coordinates,

$$ds^2 = -f(r)dt^2 + f^{-1}(r)dr^2 + r^2(d\theta^2 + \sin^2 \theta d\phi^2), \quad (2)$$

where  $f(r) = 1 - 2M/r$ . The scale factor in the Friedmann domain is,

$$a(\eta) = \frac{1}{2}a_m(1 + \cos \eta) \quad (3)$$

with  $a_m$  denoting its initial value (which is also the maximum value). The surface of the star is labelled as  $\chi_o$  and  $R$  in these two coordinate frames and as seen in Schwarzschild coordinates is moving inwards as a timelike radial geodesic

with zero initial velocity at some distance  $R_i$  corresponding to the initial stellar radius at the onset of collapse. This translates into

$$R(\eta) = \frac{1}{2}R_i(1 + \cos \eta) . \quad (4)$$

The relation between the two different time coordinates is given by

$$t = 2M \ln \left| \frac{(R_i/2M - 1)^{1/2} + \tan(\eta/2)}{(R_i/2M - 1)^{1/2} - \tan(\eta/2)} \right| + 2M(R_i - 1)^{1/2}[\eta + (R_i/4M)(\eta + \sin \eta)] . \quad (5)$$

Note that the conformal time coordinate  $\eta$  is restricted between  $\eta = 0$  (initial time when collapse begins) and  $\eta = \pi$  at which moment the star has shrank to zero radius. Of course, the physically relevant value  $\eta_c$  for  $\eta$  is the time when the star is crossing its Schwarzschild radius,

$$\eta_c = \arccos \left( \frac{4M}{R_i} - 1 \right) . \quad (6)$$

The initial stellar radius as measured in units of the stellar total mass  $M$  is,

$$\frac{R_i}{M} = 2 \sin^{-2} \chi_o . \quad (7)$$

The parameter  $\chi_o$  can take any value between 0 ( $R_i/M \rightarrow \infty$ ) and  $\pi/2$  ( $R_i/M = 2$ ). A typical collapsing object has  $R_i \sim 10^4 - 10^5 M$  (the size of a white dwarf), and this value can rise even higher for supermassive stars.

## B. The scalar wave equation in the field of a collapsing star

As we mentioned earlier in this paper, we shall consider the simplest possible case of perturbations, i.e. a massless scalar field  $\Phi$ , which obeys the covariant wave equation  $\nabla^\alpha \nabla_\alpha \Phi = 0$ . We can immediately separate the angular dependence by means of the decomposition

$$\Phi = \sum_{\ell,m} R_{\ell m} Y_{\ell m}(\theta, \phi) . \quad (8)$$

In the Friedmann domain (also simply termed “interior” hereafter), the wavefunction  $R_{\ell m}$  can be rescaled as

$$R_{\ell m}(\eta, \chi) = \frac{\psi_{\ell m}(\eta, \chi)}{a(\eta) \sin \chi} . \quad (9)$$

Note that by this operation we have isolated the usual “adiabatic” change  $\sim a^{-1}$  due to the contracting background. The new wavefunction  $\psi$  satisfies (for brevity we drop the  $\ell, m$  subscript hereafter),

$$\partial_\eta^2 \psi - \partial_\chi^2 \psi + V(\eta, \chi) \psi = 0 , \quad (10)$$

where the effective potential  $V$  is given by (for  $\chi \leq \chi_o$ ),

$$V(\eta, \chi) = \frac{\ell(\ell+1)}{\sin^2 \chi} - 1 - \frac{\ddot{a}}{a} = \frac{\ell(\ell+1)}{\sin^2 \chi} - \frac{1}{2} \cos^{-2}(\eta/2) . \quad (11)$$

Similarly, for the Schwarzschild domain (to be called “exterior”) we have,

$$R(t, r) = \frac{1}{r} \psi(t, r) \quad (12)$$

with  $\psi$  satisfying the familiar Regge-Wheeler equation,

$$\partial_t^2 \psi - \partial_{r_*}^2 \psi - V(r) \psi = 0 \quad (13)$$

with

$$V(r) = f(r) \left( \frac{\ell(\ell+1)}{r^2} + \frac{2M}{r^3} \right) , \quad (14)$$

and where  $r_*$  is the so-called “tortoise” radial coordinate defined by  $dr_*/dr = 1/f(r)$ .

Naturally, our attention will be mainly focused on the interior time-dependent field which is identical (by construction) to the field of a closed Friedmann model. The exterior field is of little concern to us, as it is responsible for effects like the quasinormal mode ringing and late time power-law tails which are the expected (and well studied) dominant components of the emitted signal at the final stages of a realistic collapse scenario.

As a warm up, we first consider the initial value problem for the wave equation (10) in a pure Friedmann gravitational field. Moreover, we restrict ourselves to the monopole case  $\ell = 0$ . Assuming static initial data  $\psi(0, \chi) = \psi_o(\chi)$ ,  $\partial_\eta \psi(0, \chi) = 0$  and imposing the additional boundary condition  $\psi(\eta, \pi) = 0$ , the general solution of (10) is given by,

$$\psi(\eta, \chi) = \frac{2}{\pi} \sum_{n=1}^{+\infty} \sin(n\chi) \int_0^\pi d\chi \psi_o(\chi) \sin(n\chi) \left[ \cos(n\eta) + \frac{1}{2n} \tan(\eta/2) \sin(n\eta) \right] . \quad (15)$$

The key feature of eqn. (15) is the term  $\sim \tan(\eta/2)$ . This term originates from the  $\ddot{a}/a$  term in the potential eqn. (11) and consequently encodes all the effects associated with the time variance of the background gravitational field. We can apply the solution (15) for initial data of the form of a narrow Gaussian pulse. The resulting field is shown in Fig. 1.

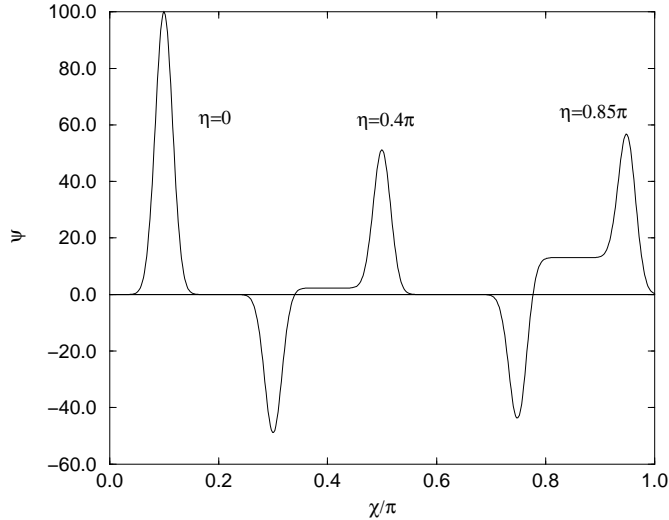


FIG. 1. Scalar field propagation in Friedmann spacetime. The initial field is shown on the left and later “snapshots” are shown on the center of the figure ( $\eta = 0.4\pi$ ) and on the right ( $\eta = 0.85\pi$ ).

The field initially evolves as in flat spacetime, but at later times, we clearly observe a growth in the amplitude which is more pronounced in the “wake” behind the travelling pulse. This wake is mainly comprised of low-frequency waves (which “feel” more strongly the background gravitational field) as opposed to the main pulse which includes the higher frequency contribution. As  $\eta$  approaches  $\pi$  the field becomes enormous as compared to its initial amplitude and eventually diverges, as predicted by eqn. (15). This behaviour is a typical example of parametric amplification in Friedmann spacetime.

### C. Pushing the simplification further

Let us now return to the O-S model. The difference in the field evolution from the preceding picture is obvious: the field, as it propagates outwards, will reach the stellar surface at  $\chi_o$ . Once there, it will partially transmit to the exterior and partially reflect back to the interior (see Fig. 2). In principle, one could try and describe such a process analytically, by making some simplifications for the exterior field (for example, by keeping only the centrifugal term in the potential). However, such an attempt soon runs into serious technical problems related to the coordinate

“discontinuity” at the stellar surface. To overcome this difficulty, one could use comoving Novikov coordinates [14] which smoothly covers the entire spacetime. However, in this case the resulting exterior wave equation is not separable, an undesired feature for any analytical work. At the same time, we should be almost certain that this coordinate-induced problems has nothing to do with the physics we try to study here.

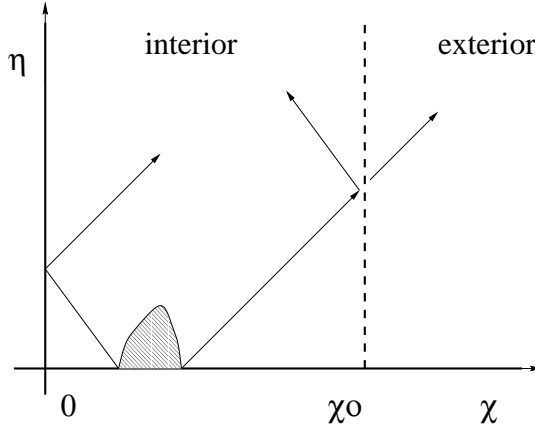


FIG. 2. A schematic illustration of our problem: Initial data placed inside a “collapsing” star propagate inwards and outwards experiencing partial and total reflections at the stellar surface ( $\chi = \chi_0$ ) and at the center ( $\chi = 0$ ) respectively.

Of particular relevance to this point is the recent study by Laarakkers and Poisson [15] on scalar wave propagation in the so-called Einstein-Strauss spacetime. This spacetime is, as the O-S model, a combination of Schwarzschild and Friedmann geometries but patched in the opposite sense with the interior being Schwarzschild and the exterior Friedmann. Apart from providing fully numerical results, these authors considered a simple toy-equation that closely resembles the pair of exact wave equations (10), (13). The construction was based on simply replacing eqns. (10),(13) with a single wave equation by extending the Friedmann coordinates over the entire spacetime. It was shown that the simplified wave equation captures most of the effects present in wave propagation in the Einstein-Strauss spacetime.

For the purposes of the present paper we have chosen to follow a similar path and replace eqns. (10),(13) with the toy-equation,

$$\partial_\eta^2 \psi - \partial_\chi^2 \psi + V(\eta, \chi) \psi = 0 , \quad (16)$$

where the new effective potential is,

$$V(\eta, \chi) = \begin{cases} 0 & \text{for } \chi > \chi_0, \quad \text{exterior} \\ -\frac{1}{2} \cos^{-2}(\eta/2) & \text{for } \chi \leq \chi_0, \quad \text{interior} \end{cases} \quad (17)$$

Hereafter, we shall consider only the monopole case  $\ell = 0$ . We have verified that all results presented in this paper remain qualitatively the same even for higher multipoles. The important point is that the new potential is *identical* to the “exact” O-S potential in the interior, where the phenomenon of parametric amplification would take place. On the other hand, our model is unable to describe any effects related to the exterior gravitational field, such as backscattering of outgoing waves. In principle, this last feature could be of importance, as it would lead to trapping of some portion of the initial field inside the star. For this reason, we have also considered a star whose surface fully reflects any outgoing waves (see Section IV).

In a sense, eqn. (16) describes a static star (as seen by both external and internal observers) with some kind of time-varying gravitational potential in its interior. This star, and with respect to external observers *only*, knows nothing about collapse. Physical parameters like the total duration of collapse have to be “borrowed” from the O-S model. We believe that the wave equation (16), just as in the case of Einstein-Strauss spacetime, yields reliable predictions on scalar wave dynamics.

It is possible to find an analytic solution to the above toy-equation (see [15] for a treatment of the  $k = 0$  Friedmann equivalent) that describes the first transmission/reflection of a wavepacket through the potential discontinuity. In principle, we could extend this solution to incorporate multiple transmissions/reflections for the needs of our problem. However, the resulting expression becomes increasingly messy. This is the main reason that led us to approach the problem numerically.

### III. TIME EVOLUTIONS

We have written a simple numerical code for solving eqn. (16) after prescribing some initial data (typically in the form of a Gaussian pulse). The code, which employs a standard leapfrog step algorithm, was tested for convergence and stability. We have widely experimented with collapsing models of different  $R_i$  and placing the initial data at different stages of the collapse. A typical example of our results for the field as observed outside the star is shown in Fig. 3. In this simulation we placed the initial data at  $\eta = 0$ , i.e. at the onset of the collapse, and centered at  $\chi = \chi_o/2$ , while the initial radius is  $R_i = 10^4 M$ . We see that the field has escaped from the star, essentially unaffected, after a lapse of time of the order  $\sim 3\chi_o/2$  (which is the light time-travel for the, initially ingoing, wave component to reach the surface). Only a minute fraction of the initial field (specifically the low frequency components) has been left inside the star while  $R \gg M$ . The same scenario is repeated in Fig. 4, but now the initial data is placed at a later time  $\eta_i = 0.97\pi$ . This corresponds to an instantaneous stellar radius  $R \approx 22M$ . The final time is  $\eta_f \approx 0.99\pi$  which gives a radius  $R \approx 2.1M$ . In this case, the potential inside the star is much more pronounced and consequently is more effective in trapping inside the star a small fraction of the initial pulse for a considerable time. The majority of the field, however, escapes during the first two crossings of the stellar surface. In the same Figure we illustrate the signal from a star with a potential “frozen” at its value at  $\eta = \eta_i$  (dashed curve) and at  $\eta = \eta_f$ . We can see that the general appearance of the signal is similar for a static and non-static potential. It is very hard to say if there are any genuine features of parametric amplification present in the signal. For this reason we illustrate (see Fig. 5) the field as it looks at  $\eta = 0.998\pi$  when the stellar radius has decreased to  $R \approx 0.001M$ . An amplified field inside the star can be clearly seen now (although it could never escape to infinity). In all the situations we examined, we reached a similar conclusion. Amplification becomes notable only after the star has crossed the Schwarzschild radius. Our final time evolution concerns the appearance of the emitted field as a function of the frequency content of the initial data. This can be simply done by considering as initial data a modulated Gaussian pulse,

$$\psi_o(\chi) = \exp[-0.5(\chi - \chi_c)^2/\sigma^2] \sin[\lambda(\chi - \chi_c)] , \quad (18)$$

where  $\chi_c$  the pulse location and  $\lambda$  is the modulation frequency. In Fig. 6 we show a comparison between the signals originated by an unmodulated pulse and a pulse with  $\lambda = 20/\chi_o$ . All other parameters are the same to the ones of Fig. 4. As we should have expected, the high-frequency pulse is escaping from the star more easily, and the late time “tail” is strongly suppressed.

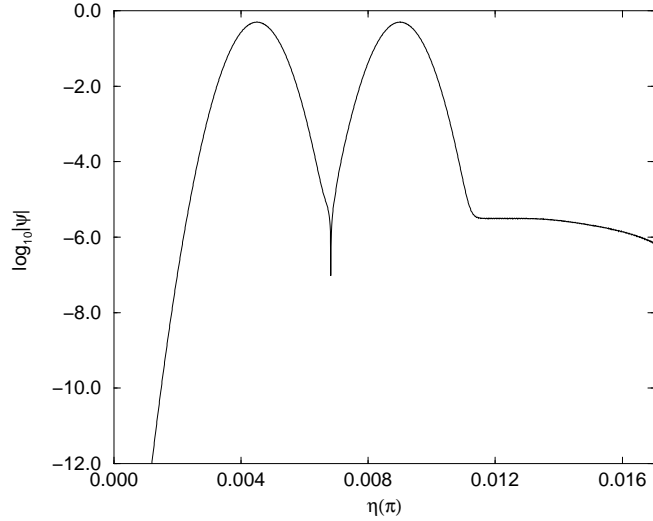


FIG. 3. The field as observed at the radial location  $\chi = 1.5\chi_o$ , for  $R_i = 10^4 M$ . The initial pulse was placed at  $\chi_o/2$  and  $\eta = 0$ .

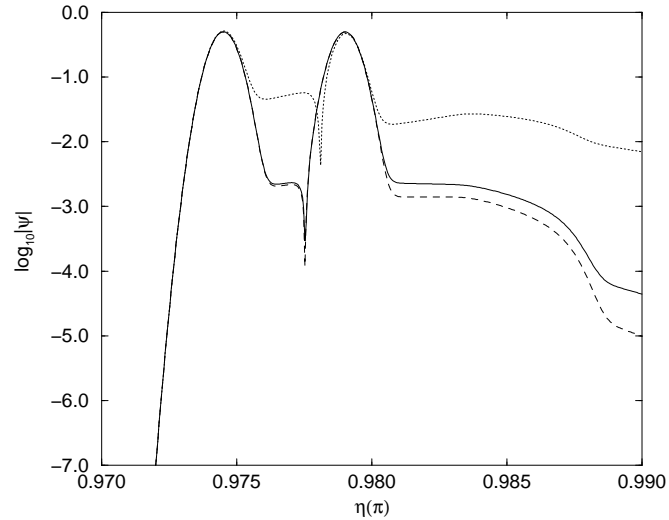


FIG. 4. The field (solid curve) as observed at  $\chi = 1.5\chi_0$ , for  $R_i = 10^4 M$ . The initial pulse was placed at  $\eta_i = 0.97\pi$  (corresponding to a radius  $R \approx 22M$ ). The dashed and dotted curves depict the field for a “frozen” static potential  $V(\eta = \eta_i)$  and  $V(\eta = \eta_f)$  respectively.

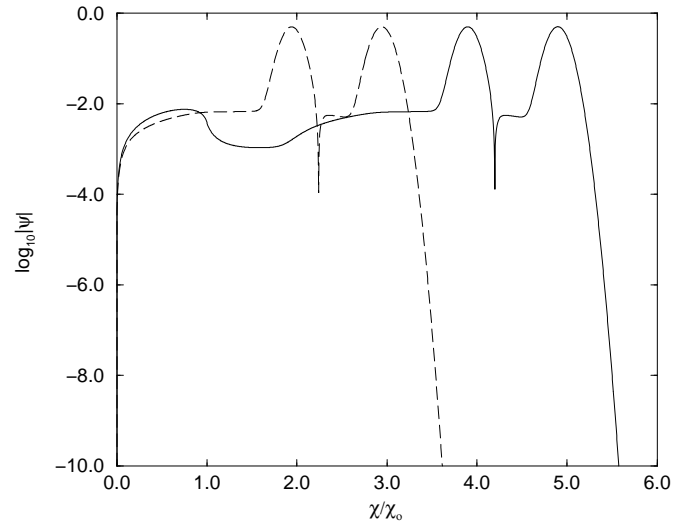


FIG. 5. “Snapshots” of the field at time  $\eta = 0.9998\pi$  (solid curve) corresponding to a radius  $R \approx 0.001M$  and at  $\eta = 0.99\pi$  (dashed curve) corresponding to  $R \approx 2M$ . In the former, it is easy to distinguish the amplified field in the stellar interior. The initial radius is  $R_i = 10^4 M$ , and the initial data were placed at  $\eta_i = 0.98\pi$ .

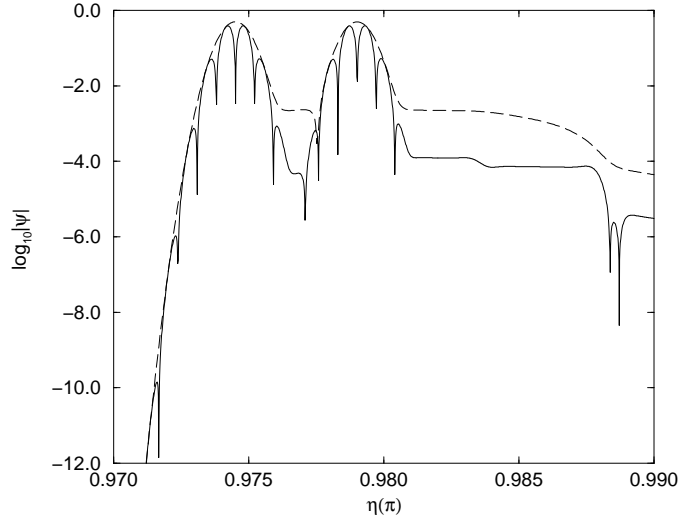


FIG. 6. Dependence of the observed signal (at  $\chi = 1.5\chi_o$ ) on the frequency content of the initial data: the dashed (solid) curve was generated by a “simple” (modulated) Gaussian pulse as initial data. It is obvious that high frequency components escape from the star much easier.

#### IV. A “MIRROR” STAR

The results of the previous Section are clearly not very optimistic regarding the efficiency of parametric amplification. In order to put an upper limit to this efficiency (at least for scalar perturbations) we have considered a “mirror” star, i.e. a star which totally reflects any outgoing field at the surface. Clearly, this situation is the most favoured one from the point of view of the amplification process, as the field will stay trapped inside the star for the entire collapse event.

Mathematically, this mirror star is modelled by setting the additional boundary condition  $\psi(\eta, \chi_o) = 0$ . Hence, the field inside the star has two inflection points at  $\chi = 0, \chi_o$ . It is straightforward to find an analytic solution to this problem that also satisfies static initial data  $\psi(0, \chi) = \psi_o(\chi)$  (see Appendix A for details),

$$\psi(\eta, \chi) = \frac{2}{\chi_o} \sum_{n=1}^{+\infty} C_n \sin(n\pi\chi/\chi_o) \left[ \cos(n\pi\eta/\chi_o) + \frac{\chi_o}{2n\pi} \tan(\eta/2) \sin(n\pi\eta/\chi_o) \right], \quad (19)$$

where

$$C_n = \int_0^{\chi_o} d\chi \psi_o(\chi) \sin(n\pi\chi/\chi_o). \quad (20)$$

We can strictly quantify the amplification of the field by means of the total energy

$$E = \frac{1}{2} \int_0^{\chi_o} d\chi \left[ (\partial_\eta \psi)^2 + (\partial_\chi \psi)^2 + V \psi^2 \right]. \quad (21)$$

It can be easily shown (see Appendix B) that

$$E(\eta) - E(0) = \frac{1}{2} \int_0^\eta \int_0^{\chi_o} d\eta' d\chi \psi^2 \partial_{\eta'} V. \quad (22)$$

In this simple way we can see that the field energy is not conserved due to the time-varying potential.

Combining eqn. (19) with eqn. (22), we can monitor the energy of the scalar field inside the collapsing star. Results of this calculation, for a selection of  $R_i$ , are shown in Fig. 7, where we plot the quantity  $\log_{10} |100 \times \{E(\eta) - E(0)\}/E(0)|$  (i.e. the percentage fractional change in the energy) as a function of  $\eta$ . The conclusion from this calculation is rather disappointing from an “observational” point of view: The amplification factor is  $\sim 1\%$  when the star is about to

cross its Schwarzschild radius. It only becomes important, at later times, when the radius is close to zero. This is in agreement with the behaviour seen in the time-evolutions in the field of a “transparent” star (Section III). According to Fig. 7, there is a  $\sim 10\%$  amplification when  $R \sim 0.25M$ . It is interesting to note that, according to Fig. 7, the amplification factor is almost the same for a given value of  $R$  and different  $R_i$ . An intuitive explanation of this behaviour is given in the following Section. It is important to mention that the amplification factor at the moment of horizon crossing proved to be sensitive to the width of the initial pulse. Specifically, by decreasing the width of the pulse the amplification factor can drop down by an order of magnitude. This can be understood in terms of the fact that parametric amplification strongly depends on the frequency (see discussion in the next Section).

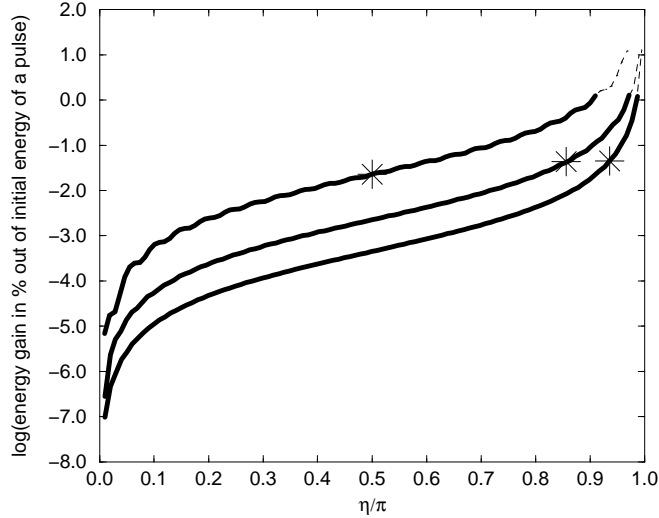


FIG. 7. Setting an upper limit for the amplification factor: We plot the percentage fractional amplification as a function of time. Three different initial radii are shown:  $R_i = 100M$  (top curve),  $R_i = 1000M$  (middle curve) and  $R_i = 5000M$  (bottom curve). Different stages of the collapse can be distinguished in the following way: The solid curves terminate at the points that correspond to horizon crossing by the stellar surface ( $R = 2M$ ). The dashed curves continue down to  $R \approx 0.25M$ . The stars denote the times where the star has a radius  $R = 50M$ .

In Fig. 8 we show snapshots of the field itself inside the “mirror” star. The field evolves in a fashion similar to a standing wave (there are two main pulses repeatedly bouncing at the left and right boundaries). It is only at the very late stages ( $\eta \approx \pi$ ) that amplification can be clearly seen, in agreement with the previous energy considerations.

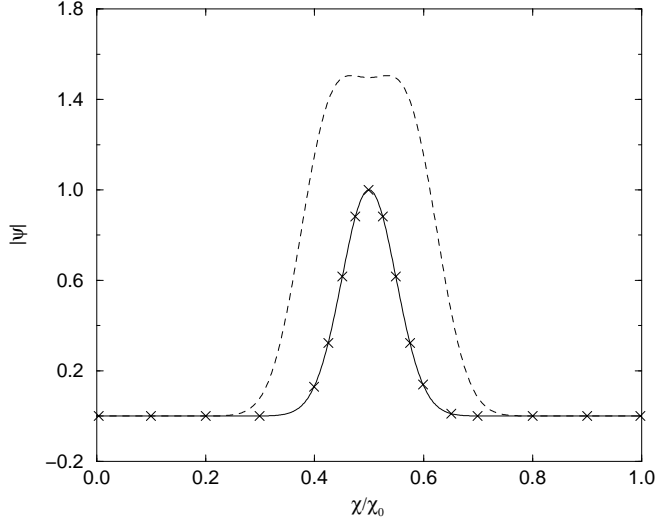


FIG. 8. Different “snapshots” of scalar field propagating inside a “mirror” star. The initial radius of the star is  $R_i = 100M$ . The initial pulse is plotted with a solid curve, the field at  $\eta = 0.7\pi$  (at which moment has reached the maximum value) is denoted by crosses, and finally, the strongly amplified field at  $\eta = 0.998\pi$  is denoted by the dashed curve.

## V. A PHYSICAL INSIGHT

In this Section we give some physical arguments which will clarify the apparent inefficiency of parametric amplification. Let us discuss first what happens in the case of cosmological perturbations. There, we have two parameters which regulate the strength of parametric amplification: the wavelength  $\lambda$  of the perturbation and the Hubble radius  $R_H \equiv a/\dot{a}$ . It is well known [11] that amplification is more efficient for large, “superhubble” modes, i.e.  $\lambda > R_H$ . This is easily understood, as it is a general property of wave propagation in a gravitational field that long wavelengths are the ones that are dominantly affected (an example is provided by Fig. 6).

In the case of a collapsing “mirror” star, there is a third lengthscale entering the problem, namely, the size  $\chi_o$  of the star. As evident from the solution (19), the field inside the star is made of the discrete spectrum  $\lambda_n = 2\chi_o/n$ . Hence, the maximum wavelength is just equal to the diameter of the star. For amplification to be significant, we should demand that,

$$\chi_o > \frac{1}{2}R_H = \frac{1}{2\tan(\eta/2)} . \quad (23)$$

Moreover, there is another restriction set by the time required for the star to cross its Schwarzschild radius. The condition  $R \geq 2M$ , with the help of eqns. (4),(7), gives,

$$\chi_o < \frac{\pi - \eta}{2} . \quad (24)$$

Conditions (23) and (24) are plotted together in Fig. 9 for various values of  $\chi_o$ , or equivalently, of  $R_i/M$ . For a given choice of  $R_i/M$  there is an amplification “window” where there is at least one superhubble mode present. At this point we also need some input from the energy expression (22), which says that the time-derivative of the potential is a crucial factor for amplification. Since  $\partial_\eta V \sim \sin(\eta/2)/\cos^3(\eta/2)$  we could argue that amplification should become stronger as  $\eta \rightarrow \pi$ . In the same limit, and according to Fig. 9, the amplification window shrinks considerably. In effect these two counter-balancing factors produce an almost uniform total amplification factor as it was shown in Fig. 7. On the other hand, for the case of pure Friedmann spacetime the corresponding window is significantly larger, which explains why amplification can be much stronger (as illustrated in Fig. 1).

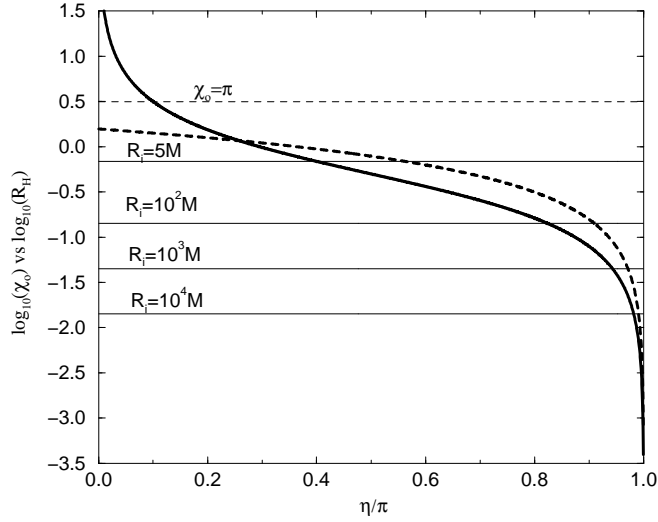


FIG. 9. The amplification “window”. The thick solid line corresponds to one half the “Hubble radius”  $R_H$  as function of time, and each thin solid line represents the comoving radius of the star  $\chi_o(R_i)$ . The thin dashed line is plotted for  $\chi_o = \pi$  which corresponds to a pure closed Friedmann spacetime. Finally, the thick dashed line is defined by eqn. (24) and represents the moment of time that the Schwarzschild horizon is crossed, for the different  $R_i/M$ .

## VI. CONCLUDING DISCUSSION

We have presented the results of an investigation on the possibility of having parametrically amplified perturbations during gravitational collapse. We have argued, based on the similarity between the time-varying gravitational field in the interior of a spherically collapsing star and the field of the closed Friedmann cosmological model, why this process will be present, at least in principle. Indeed, our investigation revealed that the process *is* present, and in order to obtain a quantitative estimate of the effect, we have constructed a simplified collapse model (which captures the physics relevant to the problem) and studied time-evolutions of a scalar field placed inside the star. We have found that, unless the star has shrunk to a radius smaller than the Schwarzschild limit, the scalar field escapes from the star in a very short timescale for amplification to become important. We have also quantified the amplification in terms of the field energy, and set an upper limit (for scalar perturbations) by considering a perfectly reflecting star, i.e. a star that keeps the field trapped in its interior for the entire collapse event (this is what we called a “mirror” star). Unfortunately, we found that even under these very favourable conditions, amplification is only of order  $\sim 1\%$  when the stellar surface is about to cross the star’s Schwarzschild radius. It is only when the radius has shrunk to a much lower value that amplification becomes notable (for example, there is a  $\sim 10\%$  amplification in the energy when  $R = 0.25M$ ). Moreover, these results remain almost invariant for a wide range of initial radii  $R_i/M$ . We have given a simple physical argument, based on the comparison between the stellar radius, the Hubble radius  $a/\dot{a}$  and the moment at which the star crosses its Schwarzschild radius, to “explain” the low efficiency of the process.

The results presented in this paper should encourage one to adopt a pessimistic point of view regarding the astrophysical importance of parametric amplification during gravitational collapse. However, this statement is far from being definite and must be viewed with some caution. We have considered one of the simplest possible models to describe a collapsing star. One could naturally ask how the above conclusion may change when more realistic models are adopted (which would incorporate features like pressure gradient, rotation etc.). In all these models, there is still present a time-varying background gravitational field which could pump energy into any kind of perturbations inside the star. There is no way at this point to say whether the amplification mechanism would operate with the same efficiency as in pressureless spherical collapse. Some steps towards including rotational effects could be taken by considering a slowly rotating O-S collapse model [17]. There are also other factors that should be taken into account in realistic collapse. For example, it is well established [16] that an inhomogeneous collapsing star can easily give birth to a naked singularity instead of a black hole. Under such conditions, our results suggest that strongly amplified fields could be generated while the stellar radius is  $< M$ , and subsequently escape to infinity. In our view, and despite the “negative” results of this study, further (and more detailed) work is needed to give a more complete answer on the astrophysical significance of parametric amplification.

## ACKNOWLEDGMENTS

We are grateful to L.P. Grishchuk for providing the idea that initiated this work and for many helpful discussions. We would also like to thank N. Andersson, C. Gundlach, J. Inglesfield and B.S. Sathyaprakash for useful discussions/comments.

## APPENDIX A: ANALYTIC SOLUTION FOR THE “MIRROR” STAR

In this Appendix we derive the analytic solution used to describe a scalar field inside the “mirror” star of Section IV. We rewrite eqn. (16),

$$\partial_\eta^2 \psi - \partial_\chi^2 \psi + V(\eta, \chi) \psi = 0$$

and perform separation of variables:

$$\psi(\eta, \chi) = H(\eta)X(\chi). \quad (\text{A1})$$

We then get the following pair of equations for  $H$  and  $X$ ,

$$\partial_\eta^2 H + \left[ \nu^2 - \frac{1}{2} \cos^{-2}(\eta/2) \right] H = 0, \quad (\text{A2})$$

$$\partial_\chi^2 X + \left[ \nu^2 - \frac{\ell(\ell+1)}{\sin^2(\chi)} \right] X = 0. \quad (\text{A3})$$

where  $\nu$  is the separation constant. The solution of these equations is,

$$X_\nu(\chi) = c(\nu, l) \sqrt{\sin(\chi)} P_{\nu-\frac{1}{2}}^{-l-\frac{1}{2}}[\cos(\chi)], \quad (\text{A4})$$

$$H_\nu(\eta) = c_1(\nu)u_1(\nu, \eta) + c_2(\nu)u_2(\nu, \eta), \quad (\text{A5})$$

where  $c, c_1, c_2$  are constants (with respect to  $\eta$  and  $\chi$ ),  $P_\kappa^\mu[z]$  are associated Legendre functions and

$$u_1 = \cos[\nu(\pi - \eta)] - \frac{1}{2\nu} \tan(\eta/2) \sin[\nu(\pi - \eta)], \quad (\text{A6})$$

$$u_2 = 2\nu \sin[\nu(\pi - \eta)] + \tan(\eta/2) \cos[\nu(\pi - \eta)]. \quad (\text{A7})$$

The above solutions already incorporate the “left” boundary condition  $\psi(\eta, 0) = 0$ .

At this point, we restrict our attention to the monopole case ( $\ell = 0$ ) only. The time dependence of the field  $\psi$  (as given by eqn. (A2) is the same irrespective of  $\ell$ , so consideration of  $\ell \neq 0$  will just overcomplicate the analysis without providing any new physical information.

We next impose the “right” boundary condition,  $\psi(\eta, \chi_0) = 0$ . For  $\ell = 0$  we find the following eigenvalues and eigenfunctions:

$$\begin{aligned} \nu_n &= \frac{\pi}{\chi_0} n, \quad \text{for } n = \pm 1, \pm 2, \dots \\ \psi_n &= [c_1(\nu_n)u_1(\nu_n, \eta) + c_2(\nu_n)u_2(\nu_n, \eta)] \sin\left(\frac{\pi n}{\chi_0} \chi\right). \end{aligned}$$

The full field  $\psi$  can be presented as an infinite sum of these eigenfunctions. The two remaining constants  $c_1, c_2$  can be fixed by the use of initial conditions (assumed static here). The final expression for  $\psi$  is,

$$\psi(\eta, \chi) = \frac{2}{\chi_0} \sum_{n=1}^{\infty} C_n \left[ \cos\left(\frac{\pi n}{\chi_0} \eta\right) + \frac{\chi_0}{2\pi n} \tan\left(\frac{\eta}{2}\right) \sin\left(\frac{\pi n}{\chi_0} \eta\right) \right] \sin\left(\frac{\pi n}{\chi_0} \chi\right), \quad (\text{A8})$$

where

$$C_n = \int_0^{\chi_0} d\chi \psi_0(\chi) \sin\left(\frac{\pi n}{\chi_0} \chi\right). \quad (\text{A9})$$

This solution exhibits a standing wave-like behaviour. Moreover, by setting  $\chi_0 = \pi$  it can be used to describe scalar wave propagation in a closed Friedmann spacetime. When applying (A8) in practice, we found that the  $n$ -sum is rapidly convergent (typically, no more than 20-25 terms are required).

## APPENDIX B: ENERGY “CONSERVATION” LAW FOR THE KLEIN-GORDON EQUATION

The “master” equation that governs the field  $\psi$  is a Klein-Gordon equation. Here we intend to derive a simple “energy conservation” expression for this type of equations when homogeneous boundary conditions are assumed for the field at the right and left endpoints.

Consider again eqn. (16)

$$\partial_\eta^2 \psi - \partial_\chi^2 \psi + V(\eta, \chi) \psi = 0, \quad (\text{B1})$$

where  $V(\eta, \chi)$  is an effective potential which can generally have both spatial and time dependence. Suppose that the field is confined in the region  $0 \leq \chi \leq \chi_0$  and  $\psi(\eta, 0) = \psi(\eta, \chi_0) = 0$  (as in the model of the “mirror” star of Section IV). Multiplying eqn. (B1) with  $2\partial_\eta \psi$  and making a trivial rearrangement we obtain

$$2\partial_\eta \psi \partial_\eta^2 \psi - 2\partial_\chi (\partial_\eta \psi \partial_\chi \psi) + 2\partial_\chi \partial_\eta \psi \partial_\chi \psi + 2V(\eta, \chi) \psi \partial_\eta \psi = 0.$$

This can also be written as

$$\partial_\eta [(\partial_\eta \psi)^2 + (\partial_\chi \psi)^2 + V\psi^2] - \psi^2 \partial_\eta V - 2\partial_\chi (\partial_\eta \psi \partial_\chi \psi) = 0. \quad (\text{B2})$$

Integrating eqn. (B2) from 0 to  $\chi_0$  and taking into account the boundary conditions we get

$$\partial_\eta \int_0^{\chi_0} [(\partial_\eta \psi)^2 + (\partial_\chi \psi)^2 + V\psi^2] d\chi = \int_0^{\chi_0} d\chi \psi^2 \partial_\eta V. \quad (\text{B3})$$

We define the quantity

$$E(\eta) \equiv \frac{1}{2} \int_0^{\chi_0} [(\partial_\eta \psi)^2 + (\partial_\chi \psi)^2 + V\psi^2] d\chi. \quad (\text{B4})$$

as the field’s total energy (this can be compared with the energy expression for a vibrating string). We have then shown that,

$$E(\eta) - E(0) = \frac{1}{2} \int_0^\eta \int_0^{\chi_0} d\eta' d\chi \psi^2 \partial_{\eta'} V. \quad (\text{B5})$$

In the “usual” case of time-independent potentials, this equation just says that the field energy is conserved. This property is spoiled when the potential is allowed to vary in time due to the coupling of the field and the time-derivative of the potential. This simple relation is an alternative way to view amplification of fields by time-dependent potentials.

- [1] L.P. Grishchuk, V.M. Lipunov, K.A. Postnov, M.E. Prohorov and B.S. Sathyaprakash, *Phys. Usp.* **44**, 1 (2001) [*Usp. Fiz. Nauk* **171**, 3 (2001)]
- [2] E. Müller, in O. Steiner and A. Gautschi eds., *Computational methods for astrophysical fluid flow*, Saas-Fee Advanced Course 27, 343 (Springer, 1998)
- [3] J.R. Oppenheimer and H. Snyder, *Phys. Rev.* **56**, 455 (1939)
- [4] R.H. Price, *Phys. Rev. D* **5**, 2419 (1972)
- [5] C.T. Cunningham, R.H. Price and V. Moncrief, *Astrophys. J.* **224**, 643 (1978); *ibid* **230**, 870 (1979)
- [6] E. Seidel and T. Moore, *Phys. Rev. D* **35**, 2287 (1987)
- [7] R.F. Stark and T. Piran, *Phys. Rev. Lett.* **55**, 891 (1985)
- [8] H. Dimmelmeier, J.A. Font and E. Müller, Report astro-ph/0103088.
- [9] C. Fryer, D.E. Holz and S.A. Hughes, Report astro-ph/0106113, submitted to ApJ.
- [10] J.A. Font, *Living Reviews in Relativity*, electronic journal <http://www.livingreviews.org> (2000)
- [11] L.P. Grishchuk, *Zh. Eksp. Teor. Fiz.* **67**, 825 (1974) [*Sov. Phys. JETP* **40**, 409 (1975)]; *Ann. NY Acad. Sci.* **302**, 439 (1977); L. P. Grishchuk, *Phys. Rev. D* **50**, 7154 (1994).
- [12] A. Melchiorri, M.V. Sazhin, V.V. Shulga, and N. Vittorio, *Astrophys. J.* **518**, 562 (1999); M. Tegmark and M. Zeldarriaga, *Astrophys. J.* **544**, 30 (2000); A. Dimitropoulos and L.P. Grishchuk, Report gr-qc/0010087.
- [13] L.H. Ford and L. Parker, *Phys. Rev. D* **16**, 1601 (1977).

- [14] C.W. Misner, K.S. Thorne and J.A. Wheeler, *Gravitation* (Freeman, San Francisco, 1973)
- [15] W.L. Laarakkers and E. Poisson, *Phys. Rev. D* to be published (2001); Report gr-qc/0105016.
- [16] T.P. Singh, Report gr-qc/9805066 (and references therein)
- [17] L.S. Kegeles, *Phys. Rev. D* **18**, 1020 (1978)